

Supplementary Information

## **Phytate Lithium as Multifunctional Additive Stabilizes LiCoO<sub>2</sub> to 4.6 V**

Fangchang Zhang<sup>‡ a</sup>, Ning Qin<sup>‡ a</sup>, Yingzhi Li<sup>a</sup>, Hao Guo<sup>b</sup>, Qingmeng Gan<sup>a</sup>, Chun Zeng<sup>a</sup>, Zhiqiang Li<sup>a</sup>, Zhenyu Wang<sup>a</sup>, Ruo Wang<sup>a</sup>, Guiyu Liu<sup>a</sup>, Shuai Gu<sup>a</sup>, He Huang<sup>a</sup>, Zelin Yang<sup>b</sup>, Jun Wang<sup>a</sup>, Yonghong Deng<sup>a</sup>, Zhouguang Lu<sup>\* a</sup>

a. Department of Materials Science and Engineering, Shenzhen Key Laboratory of Interfacial Science and Engineering of Materials, Southern University of Science and Technology, Shenzhen 518055, China.

Corresponding author E-mail: luzg@sustech.edu.cn

b. State Key Laboratory of Advanced Chemical Power Sources. Zunyi, Guizhou 563003, China.

‡ These authors contributed equally to this work.

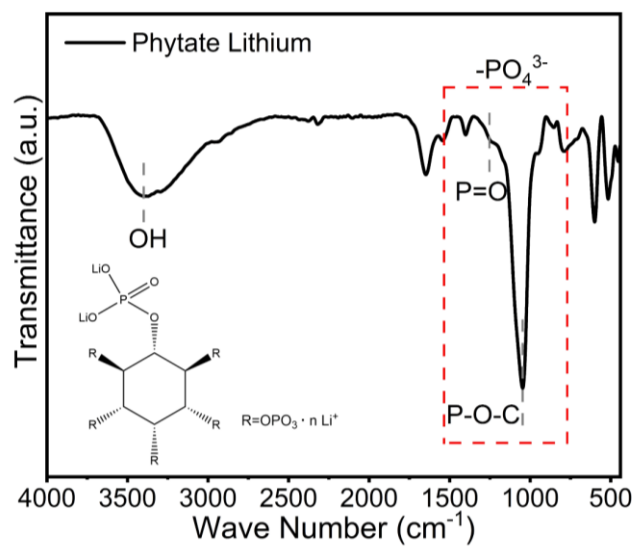


**Fig. S1** The Fourier transform infrared spectrum and inserted chemical structure of phytate lithium.

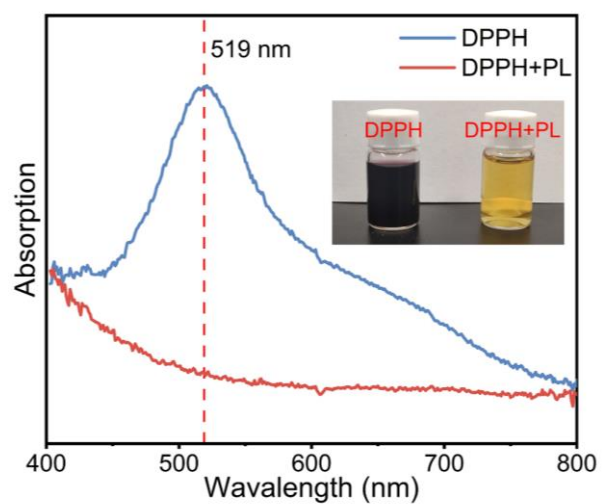


**Fig. S2** The color fading (inserted) and corresponding UV absorbance spectra of DPPH (characteristic peak at 519 nm) and DPPH+PL solutions.

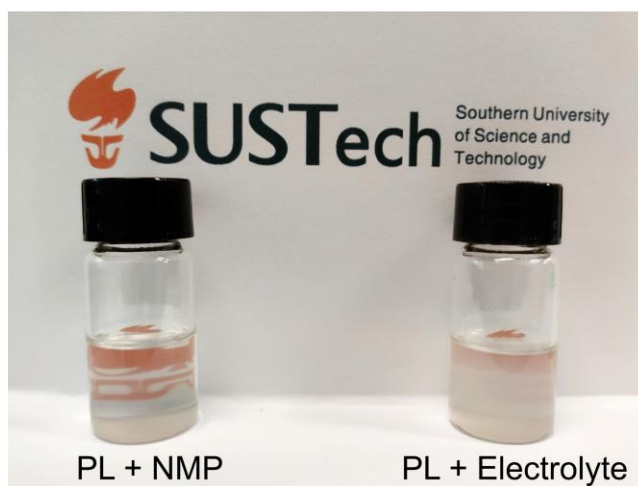


**Fig. S3** Solubility test of phytate lithium (PL) in NMP and  $\text{LiPF}_6/\text{EC}/\text{DMC}/\text{EMC}$  electrolyte.

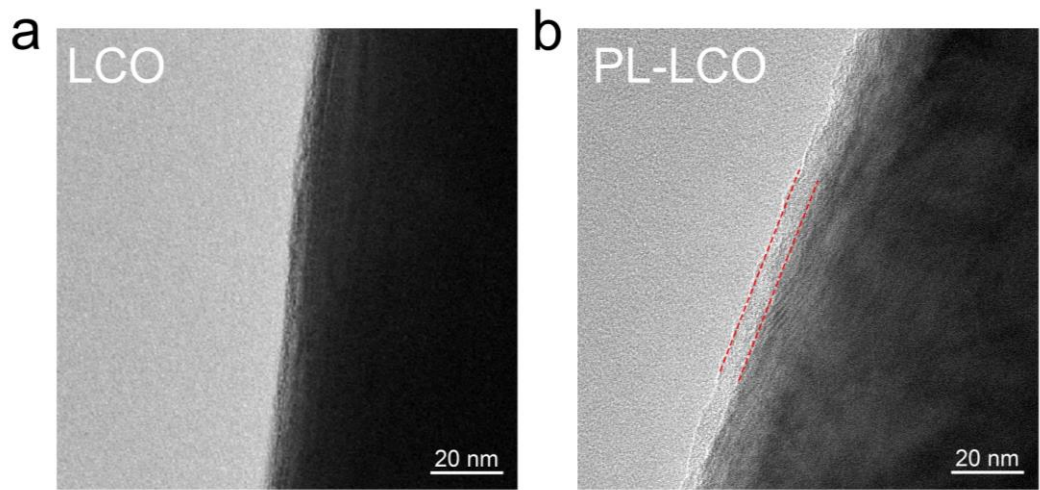


**Fig. S4** TEM images of a) LCO and b) PL-LCO before cycling.

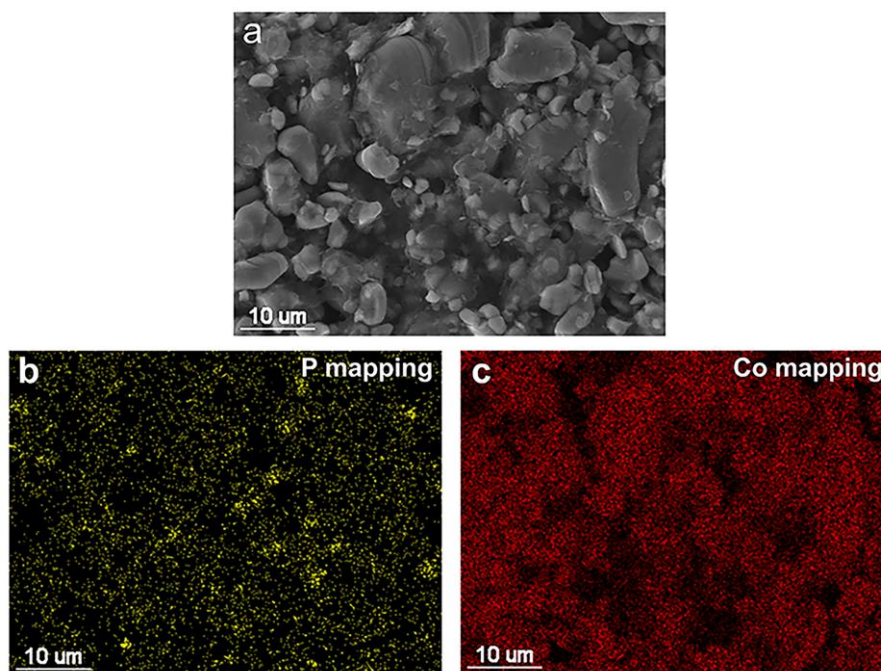


**Fig. S5** a) SEM image and b-c) EDS mapping of PL-LCO cathode.

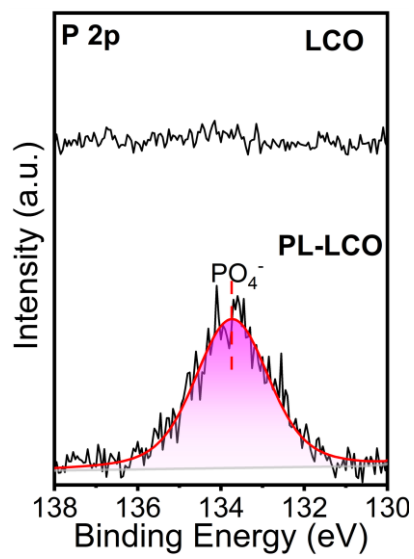


**Fig. S6** P 2p XPS spectra of LCO and PL-LCO before cycling.

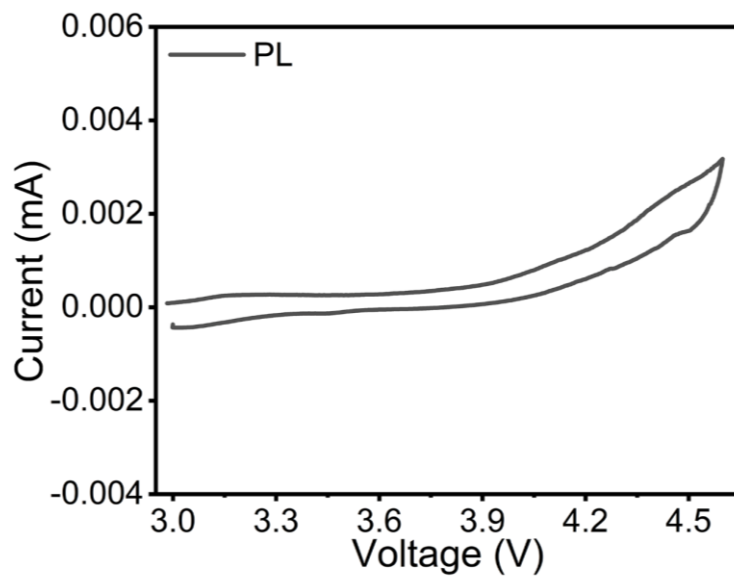


**Fig. S7** CV curve of phytate lithium at the 1<sup>st</sup> cycle with a rate of 0.1 mV/s within voltage range of 3-4.6 V.



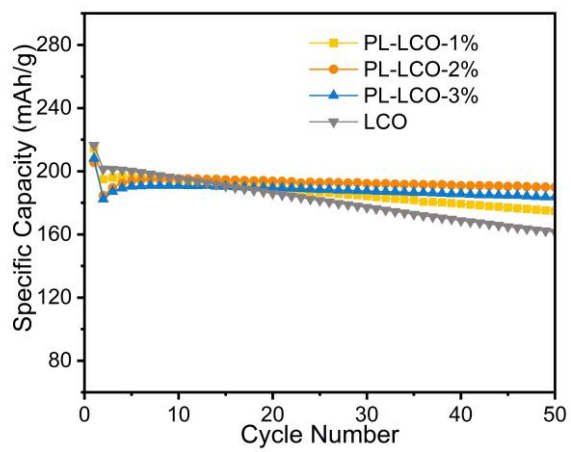


**Fig. S8** Electrochemical performance of different values of PL addition.

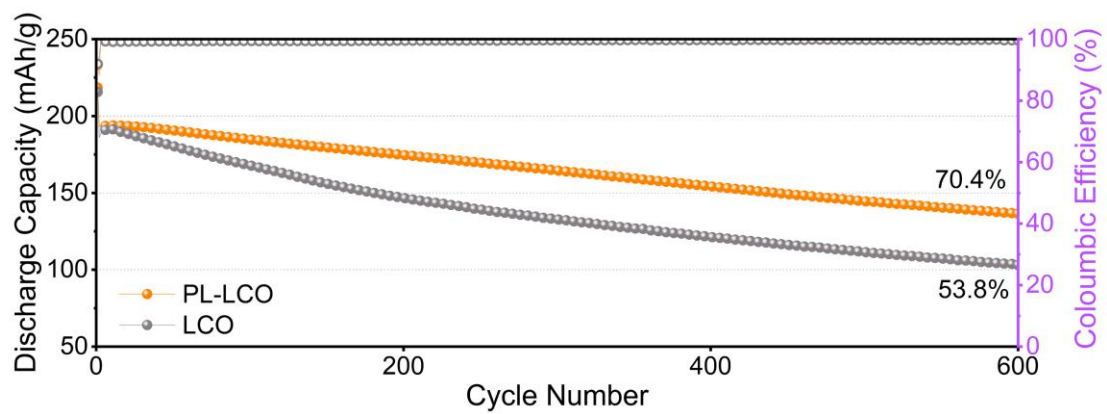


**Fig. S9** Cyclic performance of PL-LCO and LCO at a high current density of 280 mA/g for 600 cycles.

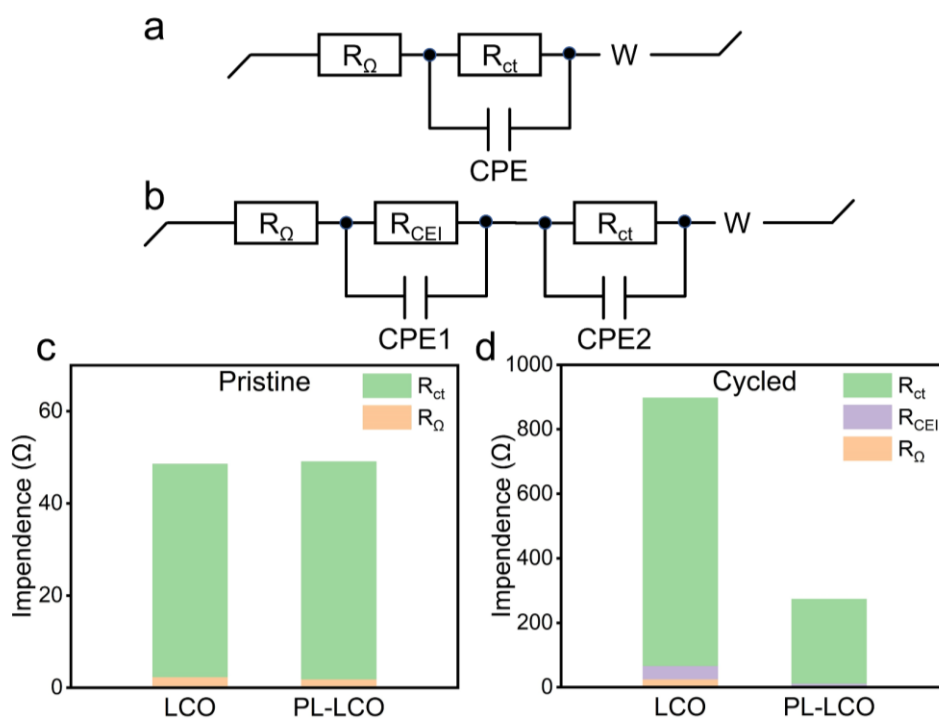


**Fig. S10** The equivalent circuit models and fitted EIS data of a,c) pristine and b,d) after 200 cycles.

**Table S1.** The fitted EIS data of LCO and PL-LCO before and after 200 cycles.

	$R_{\Omega} / \Omega$	$R_{CEI} / \Omega$	$R_{ct} / \Omega$
pristine LCO	2.415	/	46.09
pristine PL-LCO	1.927	/	47.11
cycled LCO	26.12	41.25	829.8
cycled PL-LCO	2.121	11.07	259.3

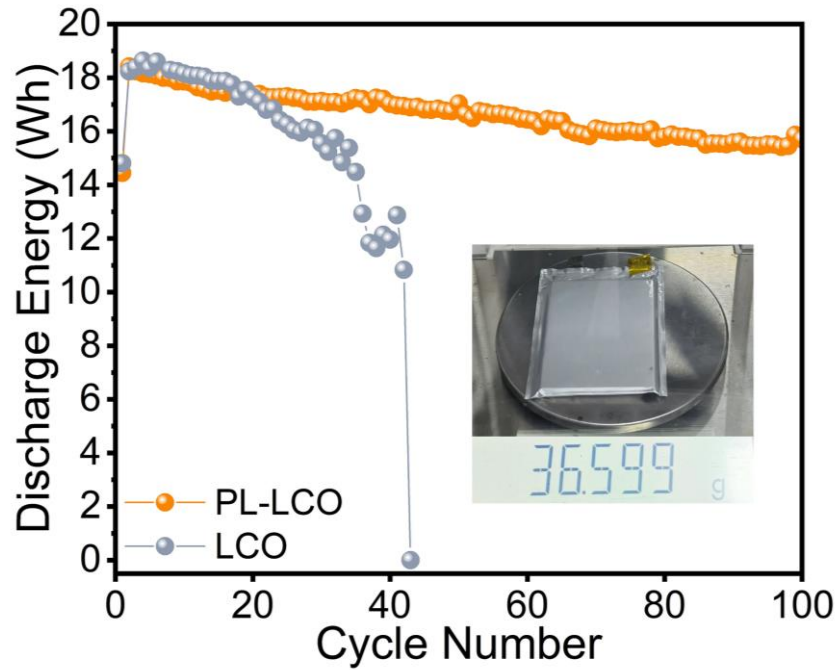


**Fig. S11** Cycling performance of 503 Wh/kg PL-LCO || Li pouch cell at a current density of 100 mA/g in the voltage range of 3 – 4.6 V.

The calculation formula for specific capacity is:

$$\text{Specific capacity (mAh/g)} = \text{capacity (mAh)} \div \text{mass of active material (g)}$$

The calculation formula for energy density is:

$$\text{Energy density (Wh/kg)} = \text{energy (Wh)} \div \text{weight of pouch cell (g)}$$

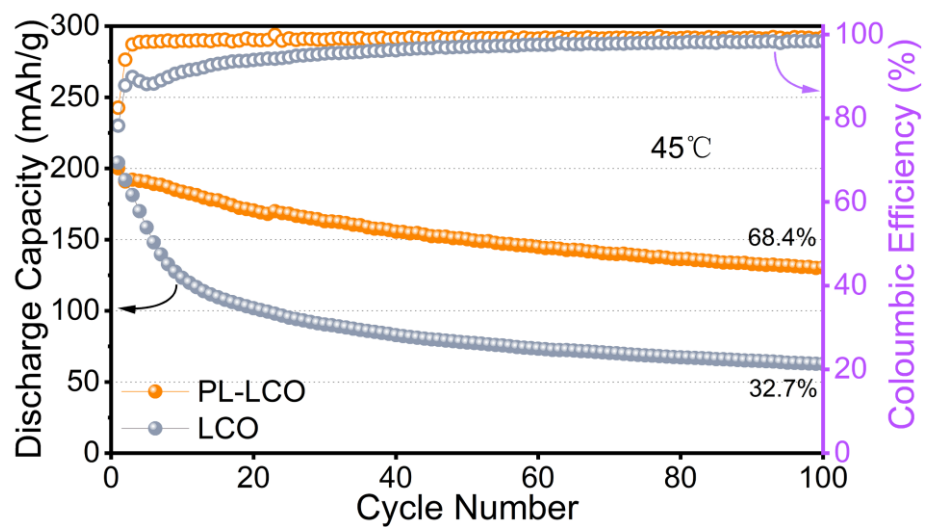


**Fig. S12** Cycling performance of LCO and PL-LCO at a current density of 140 mA/g under 45 °C.

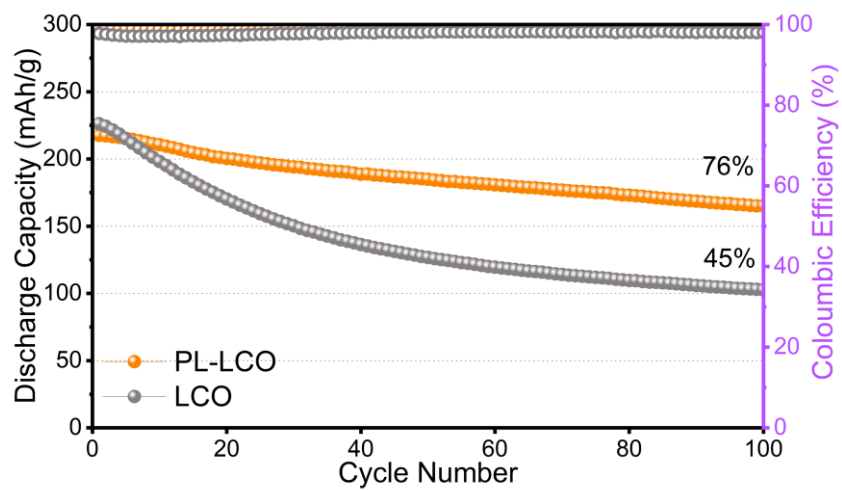


**Fig. S13** Cycling performance of LCO and PL-LCO at a current density of 140 mA/g in the voltage range of 3 – 4.65 V.

**Table S2.** Comparison of electrochemical performance of reported 4.6 V LiCoO<sub>2</sub>.

<b>Modification strategy</b>	<b>Voltage range (V)</b>	<b>Current density (mA/g)</b>	<b>Initial reversible capacity (mAh/g)</b>	<b>Capacity retention</b>	<b>Ref</b>
Li <sub>4</sub> Mn <sub>5</sub> O <sub>12</sub> coating	3-4.5	135	180.7	83% (300 <sup>th</sup> )	1
Ti, F doping	3-4.6	137	185.6	82.5% (100 <sup>th</sup> )	2
Ti, Mg, Al doping	3-4.6	137	202.3	86% (100 <sup>th</sup> )	3
Ni, Ti, Mg doping	2.7-4.6	175	180	67% (100 <sup>th</sup> )	4
Al, Nb, W doping	2.7-4.6	90	193.8	77.9% (100 <sup>th</sup> )	5
Mg doping	3-4.6	270	188	84% (100 <sup>th</sup> )	6
Al, F, Mg doping	3-4.6	137	202.6	88.4% (300 <sup>th</sup> )	7
O vacancy and V doping	3-4.6	270	170	84% (100 <sup>th</sup> )	8
LATP coating	3-4.6	137	204.2	88.3% (100 <sup>th</sup> )	9
LAF coating	3-4.6	137	200	81.8% (200 <sup>th</sup> )	10
AlZnO coating	3-4.6	185	183.9	65.7% (500 <sup>th</sup> )	11
3-TPIC electrolyte additive	3-4.6	100	186	81% (150 <sup>th</sup> )	12
VC and KBF <sub>4</sub> dual additive	3-4.6	274	182	91.1% (300 <sup>th</sup> )	13
MMD electrolyte additive	3-4.6	200	198.8	83.5% (200 <sup>th</sup> )	14
DSL binder	2.8-4.6	137	192.7	93.4% (100 <sup>th</sup> )	15
<b>This work</b>	<b>3-4.6</b>	<b>140</b>	<b>195.7</b>	<b>89.4% (200<sup>th</sup>)</b>	
		<b>280</b>	<b>195</b>	<b>70.3% (600<sup>th</sup>)</b>	
	<b>3 - 4.65</b>	<b>140</b>	<b>217.5</b>	<b>75.9% (100<sup>th</sup>)</b>	

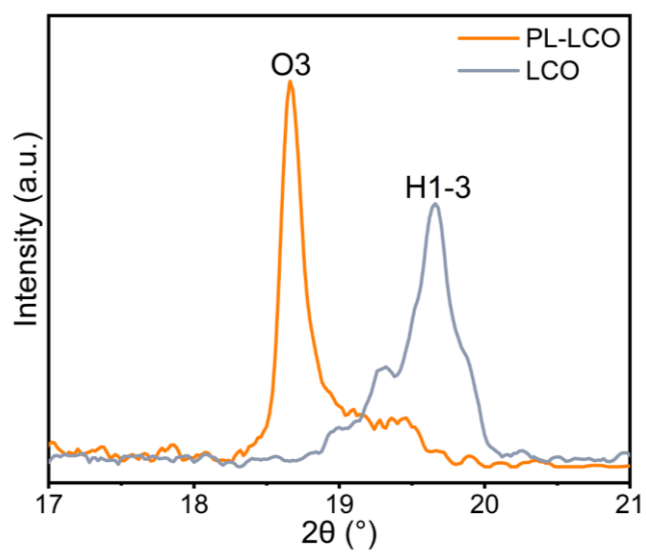


**Fig. S14** (003) XRD peak of PL-LCO and LCO at 4.6 V after CV charging until limit current decrease to beneath 0.01 mA.



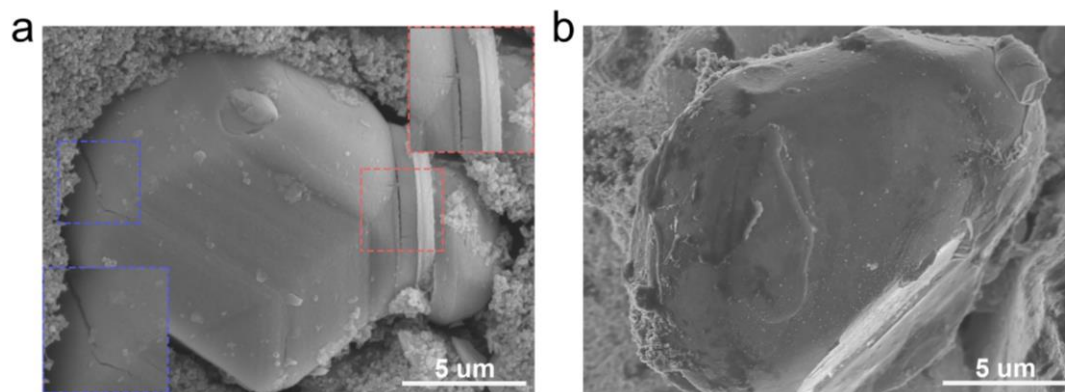


**Fig. S15** SEM images of a) LCO and b) PL-LCO after 50 cycles.

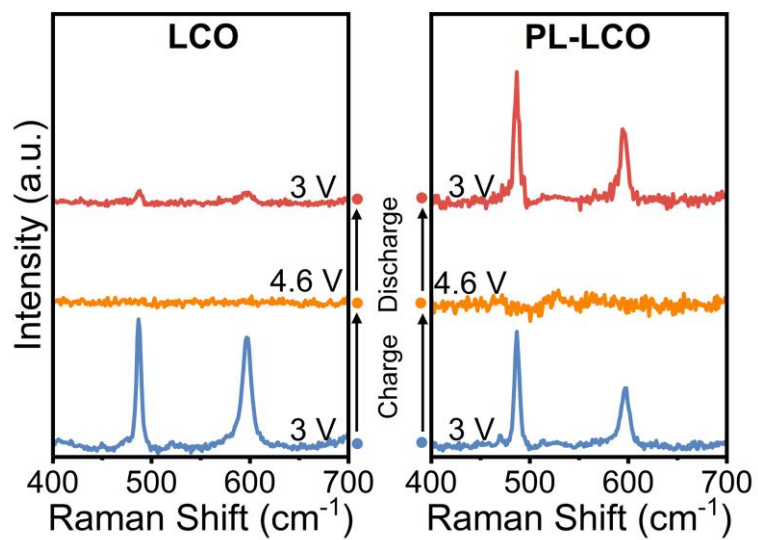


**Fig. S16** The selected curves of the  $E_g$  and  $A_{1g}$  vibrational peaks of LCO and PL-LCO at different voltages.

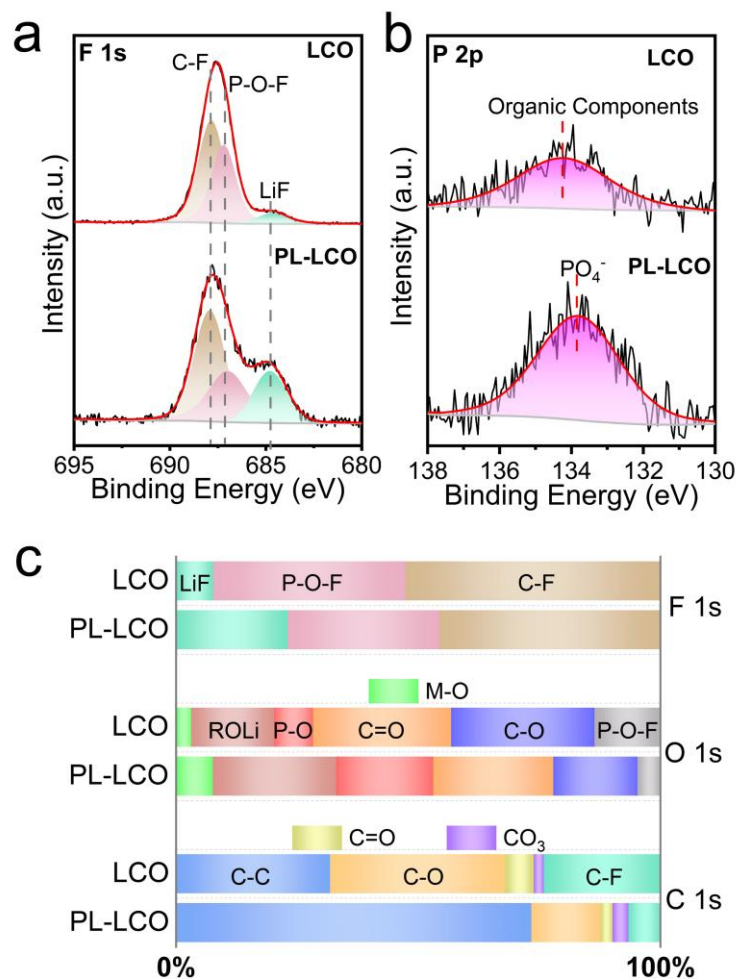


**Fig. S17** a) F 1s and b) P 2p XPS spectra of and c) the quantified chemical components of the interface layer of cycled LCO and PL-LCO after 50 cycles.

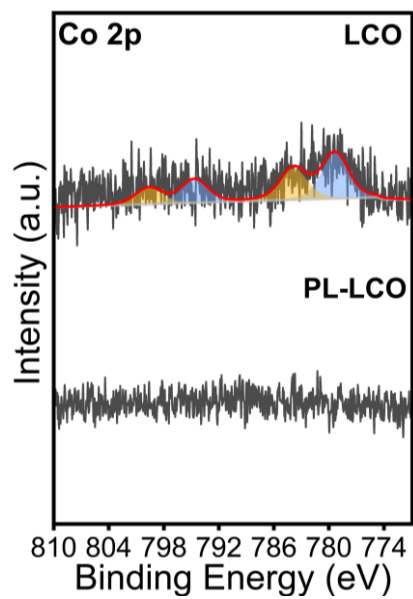


**Fig. S18** Co 2p XPS spectra collected on lithium anode of LCO and PL-LCO cells after 50 cycles.

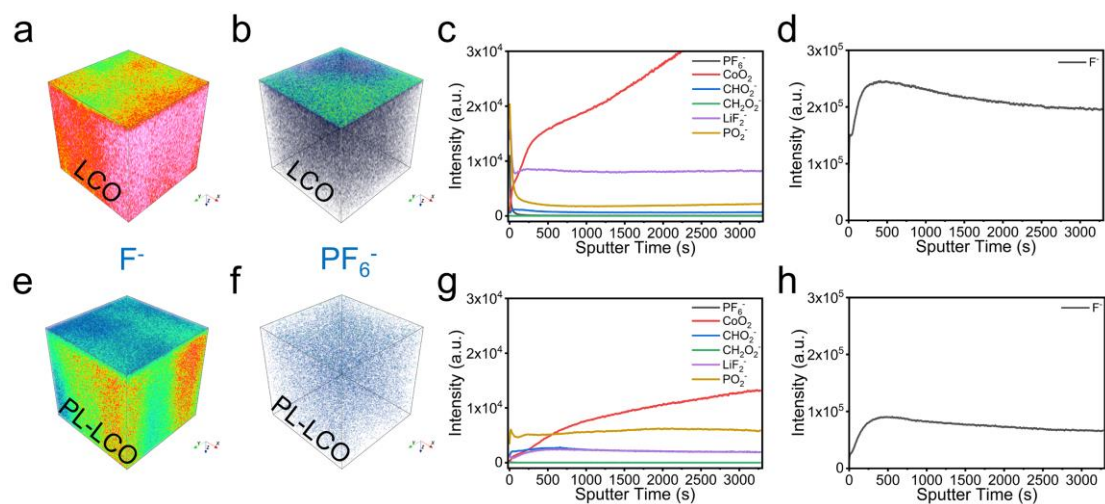


**Fig. S19** The 3D reconstruction of F<sup>-</sup> and PF<sub>6</sub><sup>-</sup> fragments at the a-b) LCO and e-f) PL-LCO cathode surface after 50 cycles. The TOF-SIMS normalized depth profiles of different fragments constituting the CEI of c-d) LCO and g-h) PL-LCO.

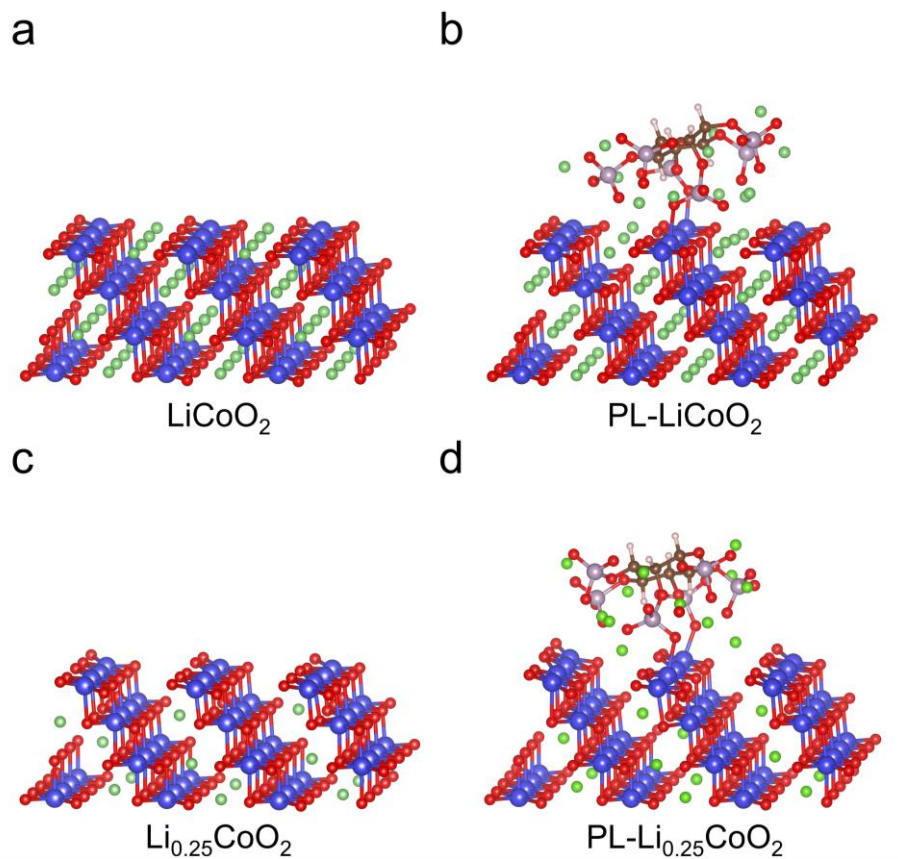


**Fig. S20** The simplified (104) surface models of LiCoO<sub>2</sub> and PL-LiCoO<sub>2</sub> at a-b) pristine state; Li<sub>0.25</sub>CoO<sub>2</sub> and PL-Li<sub>0.25</sub>CoO<sub>2</sub> at c-d) deep delithiation state.

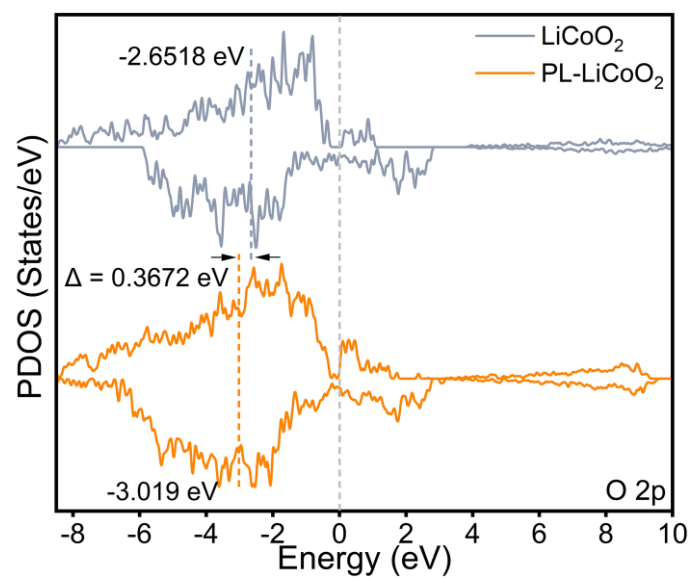


**Fig. S21** Projected density of states (PDOS) of oxygen for LiCoO<sub>2</sub> and PL-LiCoO<sub>2</sub> of (104) slab at pristine state.

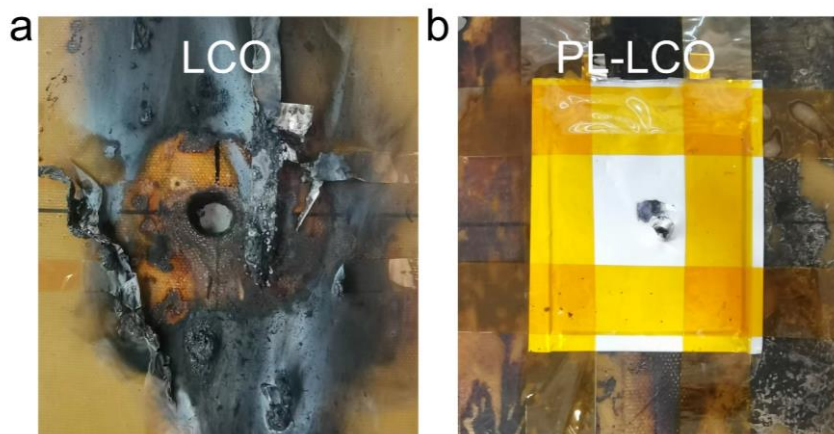


**Fig. S22** Piercing experiment of a) LCO||Li and b) PL-LCO||Li pouch cells after 100 cycles.



## Reference

1. J. Liu, J. Wang, Y. Ni, J. Liu, Y. Zhang, Y. Lu, Z. Yan, K. Zhang, Q. Zhao, F. Cheng and J. Chen, *Angew. Chem., Int. Ed.*, 2022, **61**, e202207000.
2. S. Mao, Z. Shen, W. Zhang, Q. Wu, Z. Wang and Y. Lu. *Adv. Sci.*, 2020, **9**, 2104841.
3. J. Zhang, Q. Li, C. Ouyang, X. Yu, M. Ge, X. Huang, E. Hu, C. Ma, S. Li, R. Xiao, W. Yang, Y. Chu, Y. Liu, H. Yu, X.-Q. Yang, X. Huang, L. Chen and H. Li, *Nat. Energy*, 2019, **4**, 594-603.
4. S. Song, Y. Li, K. Yang, Z. Chen, J. Liu, R. Qi, Z. Li, C. Zuo, W. Zhao, N. Yang, M. Zhang and F. Pan, *J. Mater. Chem. A*, 2021, **9**, 5702-5710.
5. S. Chen, C. Wang, Y. Zhou, J. Liu, C. Shi, G. Wei, B. Yin, H. Deng, S. Pan, M. Guo, W. Zheng, H. Wang, H. Wang, Y. Jiang, L. Huang, H. Liao, J. Li and S. Sun, *J. Mater. Chem. A*, 2022, **10**, 5295-5304.
6. Y. Huang, Y. Zhu, H. Fu, M. Ou, C. Hu, S. Yu, Z. Hu, C. -T. Chen, G. Jiang, H. Gu, H. Lin, W. Luo and Y. Huang, *Angew. Chem. Int. Ed.*, 2021, **60**, 4682-4688.
7. Y. He, X. Ding, T. Cheng, H. Cheng, M. Liu, Z. Feng, Y. Huang, M. Ge, Y. Lyu and B. Guo, *J. Energy Chem.*, 2023, **77**, 553-560.
8. W. Kong, D. Wong, K. An, J. Zhang, Z. Chen, C. Schulz, Z. Xu and X. Liu, *Adv. Funct. Mater.* 2022, **32**, 2202679.
9. Y. Wang, Q. Zhang, Z. C. Xue, L. Yang, J. Wang, F. Meng, Q. Li, H. Pan, J. N. Zhang, Z. Jiang, W. Yang, X. Yu, L. Gu and H. Li, *Adv. Energy Mater.*, 2020, **10**, 2001413.
10. J. Qian, L. Liu, J. Yang, S. Li, X. Wang, H. L. Zhuang and Y. Lu, *Nat Commun*, 2018, **9**, 4918.
11. T. Cheng, Z. Ma, R. Qian, Y. Wang, Q. Cheng, Y. Lyu, A. Nie and B. Guo, *Adv. Funct. Mater.*, 2020, **31**, 2001974.
12. J. Liu, M. Wu, X. Li, D. Wu, H. Wang, J. Huang and J. Ma, *Adv. Energy Mater.* 2023, 2300084.
13. K. Zhang, J. Chen, W. Feng, C. Wang, Y. Zhou, Y. Xia, *J. Power Sources*, 2023, **553**, 232311.
14. Y. Zou, J. Zhang, J. Lin, D. Wu, Y. Yang and J. Zheng, *J. Power Sources*, 2022, **524**, 231049.
15. H. Huang, Z. Li, S. Gu, J. Bian, Y. Li, J. Chen, K. Liao, Q. Gan, Y. Wang, S. Wu, Z. Wang, W. Luo, R. Hao, Z. Wang, G. Wang and Z. Lu, *Adv. Energy Mater.*, 2021, **11**, 2101864.